Measurements of d-d absorption spectra at low temperature

by Yoshihiro MITSUTSUKA & Ichiji KONDO***

Introduction

The temperature dependence on the visible and ultraviolet absorption band of first transition metal has hitherto been studied by many investigators.[1] And the mechanisms of their band shifts in lowering temperature, for example, the difference of Boltzmann population in their vibrational energy level between high and low temperature, the decrease in an atomic distance with a decrease in temperature, and etc. have been proposed. However, the degree of the band shifts can not be explained well with their mechanisms. The present investigation aimed to provide a explanation for more accurate mechanism.

Experimental

1. Low temperature cell

A variety of low temperature cells had been described in the literature,[2] but usually they could not be applied for our purpose because of insufficient space in the sample compartment of spectrophotometer. Therefore a new simple cell had been constructed, as shown in Fig. 1, which could be used for optical measurement between liquid

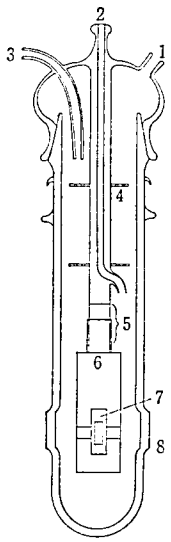

Fig. 1 Low Temperature Cell

1. Hole for electrical leads
2. Gas inlet
3. Gas outlet
4. Glass disks with holes for electrical leads
5. Koval-glass seal
6. Copper block
7. Sample
8. Windows

* 理工学部化学科助手 化学 錯体化学
** 理工学部化学科教授 化学 錯体化学

nitrogen temperature and room temperature. The pylex glass cell (diameter 60 mm, height 350 mm) had four flat windows of 20 mm diameter for the optical path. The inside wall was plated with silver to reduce radiation losses. Two windows at right angle to each other are able to be used for measurement of reflectance spectra. For evacuation and introduction of dried air, two glass tubes were attached to a cover of the cell. A copper block was suspended under the cover via Koval glass seal at the end of a glass tube (outer diameter 12 mm). A pair of heaters was attached in symmetrical position in the block. The heating element was Nichrome wire covered with ceramic tubes. This block which is screwed on can be removed and changed to an appratus for other purposes, if necessary.

2. Spectrophotometer

A Shimadzu spectrophotometer model D40-R Wide was modified by detaching the sample compartment and by exchanging a photomultiplier for HTV R406 or R446. The light source was a 10V-5A tungsten lamp or a D_2 lamp.

A light beam was focused on a sample in the copper block by a convex lens (f=50 mm) and was collected on the photomultiplier by another convex lens. When double beam operation was difficult because of a significant increase in absorbance, rough compensation could be obtained by attenuating the reference beam with a diaphragm.

3. Temperature measurement

A thermometer was constructed in hand by use of some available instruments. Fig. 2 shows the block diagram of a temperature measurement system. Various temperatures were measured with an Omega Eng. Inc. Chromel-Constantan thermocouple affixed with

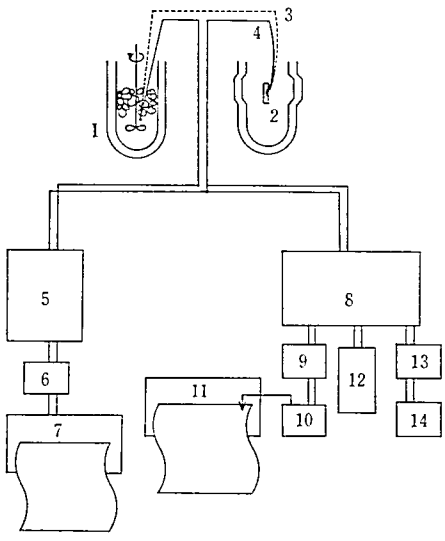

Fig. 2 Thermometer system

1. Reference junction (ice and water)
2. Measuring junction (sample)
3. Constantan, Omega (diameter 0.1 mm)
4. Chromel, Omega (diameter 0.1 mm)
5. Micro volt meter, Ohkawa-AM-2001
6. Volt ratio box
7. Recorder, Hitachi, 056-0019
8. D.C. potentiometer, Yokogawa, 2723
9. Electronic galvanometer, Yokogawa, 4931
10. OFK converter, Yokogawa, 4931
11. Recorder (Shimadzu spectrophotometer, D40-R)
12. Cadmium standard cell, Yokogawa, 2709
13. Decade resistance box, Yokogawa, 2786
14. 6V-Strong battery, Kobe, PS36

the center of a sample.

4. Materials

The common salts used were always the highest grade chemicals commercially available. Ammine complexes were prepared according to an ordinary method. A crystal was cut into a plate in about 1 mm thick and was polished well to make the surface flat. When a sample was in powder state, it was kneaded together with liquid paraffin and sandwiched between two silica plates.

5. Measurement of absorption spectra

A sample in the cell was accurately located in an optical path. The cell was filled with about 300 m*l* of liquid nitrogen and after cooling well, measurement of absorption spectra was commenced. After finishing evaporation of liquid nitrogen, temperature of a sample gradually and spontaneously elevated, and reached about 20°C in 2～3 hours. During the temperature elevation, measurements of absorption spectra were repeated at various temperature. In order to reduce the time for measurements, the copper block could be heated with the heaters. A general view of the spectrophotometer and the thermometer system is shown in Fig. 3.

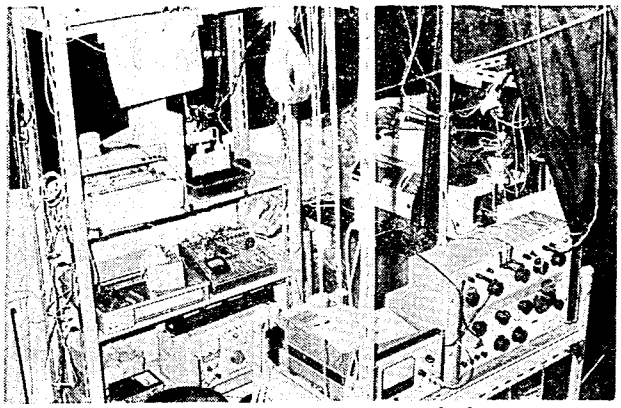

Fig. 3 General view of spectrophotometer and thermometer system.

6. Analysis of absorption curve

Observed spectra were corrected for a diffused reflection light by means of comparison with the spectrum of a substance which has no absorption band. That is, the degree of contribution of diffused reflection light to the absorption spectrum could be estimated by the spectrum of potassium alum powder. Fig. 4 shows the spectrum of potassium alum powder in 200 meshes.

Since an absorption spectra measured was mostly consisted of more than two components, they had to be separated into each components. Kuhn and Braun[9] proposed to represent the absorption curve by Gaussian error equation,

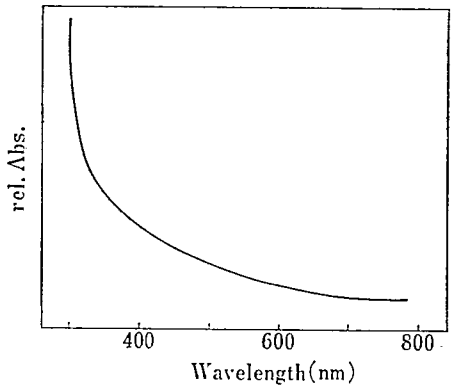

Fig. 4 Spectrum of potassium alum in 200 meshes.

$$\varepsilon=\varepsilon_{max}\exp\left[-\left(\frac{\tilde{\nu}-\tilde{\nu}_{max}}{\theta}\right)^2\right]$$

where ε and ε_{max} are the extinction coefficients at frequencies $\tilde{\nu}$ and that at the maximum frequency $\tilde{\nu}_{max}$, respectively, and θ is a constant related to the half-width of the absorption band.

The shape of observed absorption spectrum is represented by

$$A=\sum_n A_{maxn}\exp\left[-\left(\frac{\tilde{\nu}-\tilde{\nu}_{maxn}}{\theta_n}\right)^2\right]+R(\tilde{\nu})$$

where $R(\tilde{\nu})$ is the term which is independent to the absorption components of sample. It is generally impossible that the form of this function is transformed into a one-dimensional equation, for example by means of changing into logalithm. Consequently, the authors used the trial and error method for the separation of spectra. Observed spectrum was analyzed as follows.

When the shape of a absorption spectrum was observed as shown in Fig. 5, a Gaussian curve (G) was fitted to the right side of the slope in the observed curve (O. C.). The form of the equation of G was changed to another form until (O. C.) — (G) was fitted to Gaussian curve. Thus, the factors, $A_{max1,2}$, $\tilde{\nu}_{max1,2}$ and $\theta_{1,2}$ were determined to bring the observed curves and the calculated ones into the best possible agreements.

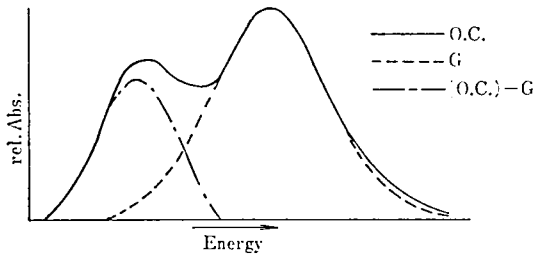

Fig. 5 A separation of an absorption curve.

Results and discussion

The experimental results and observed spectra are shown in Fig. 6～16.

Fig. 6 shows the electronic absorption spectra due to d-d transitions for $Ti_2(SO_4)_3 \cdot 8H_2O$ at room temperature and liquid nitrogen temperature. The crystal structure of $Ti_2(SO_4)_3 \cdot 8H_2O$ has not been determined, but it has been postulated from the spectrum that Ti atom is surrounded by four water molecules and two sulfate ions and that their grouping is tetragonal. The d-orbital levels[4] in crystal field of O_h and D_{4h} symmetry, with $(3Ds—5Dt) > 0$, are shown on the right of the Fig. 6. Thus, these bands are assigned to the transition of

$^2B_{1g} \leftarrow {}^2E_g$ and $^2A_{1g} \leftarrow {}^2E_g$.

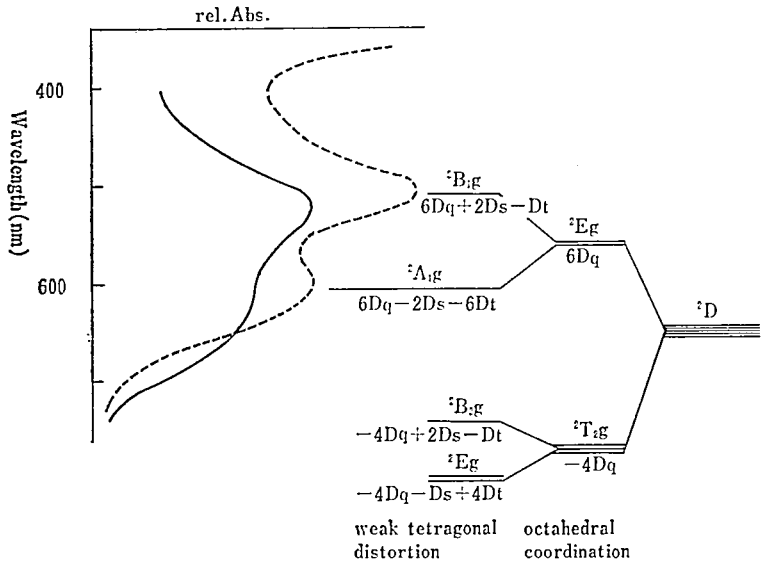

Fig. 6 Absorption spectra of $Ti_2(SO_4)_3 8H_2O$: solid line; 316 K, dotted line; 77 K; d-orbital levels in crystal fields of O_h and D_{4h} symmetry with $(3D_s—5D_t) > 0$ are shown on the right of the figure.

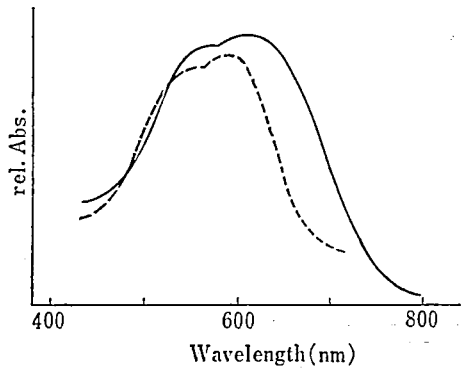

Fig. 7 Absorption spectra of $[Ti(urea)_6]$ $(ClO_4)_3$, dotted line; 77 K. solid line; 300～301 K.

Fig. 7 and Fig. 8 show the absorption spectra of $[Ti(urea)_6](ClO_4)_3$ and $CsTi(SO_4)_2 \cdot 12H_2O$, respectively. Regardless of the same ligands in the complex, the symmetry of these complexes is lowered from O_h to D_{4h} owing to Jahn-Teller effect. The aqua complex has a shoulder at the left side of absorption peak, such as a shoulder of $Ti_2(SO_4)_3 \cdot 8H_2O$. From analogy with the sulfate, the shoulder of aqua complexes may be assigned to $^2A_{1g} \leftarrow {}^2E_g$.

Fig. 9 shows the temperature dependences of the band maxima of $[Ti(urea)_6](ClO_4)_3$.

The absorption spectra of $CsV(SO_4)_2 \cdot 12H_2O$ is shown in Fig. 10. Two hands, ν_2 and ν_4 are interpreted as the spin allowed transitions $^3T_{2g}(F) \leftarrow {}^3T_{1g}(F)$ and $^3T_{1g}(P) \leftarrow {}^3T_{1g}(F)$. In addition, two weak bands which are assigned as transitions from the ground state $^3T_{1g}$ to the split components of the singlet states, appear at 11.28×10^3 cm^{-1} and 20.50×10^3 cm^{-1} (sh) which correspond to ^1E_g, $^1T_{2g} \leftarrow {}^3T_{1g}$ and $^1A_{1g} \leftarrow {}^3T_{1g}$.

Absorption maxima at 77 K and 300 K are summarized in Table 1. The calculation

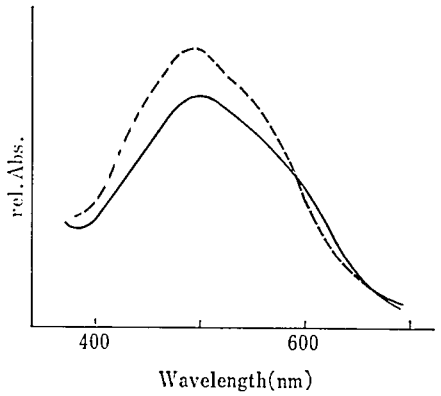

Fig. 8 Absorption spectra of $CsTi(SO_4)_2 \cdot 12H_2O$, dotted line; 77 K, solid line; 262~267 K.

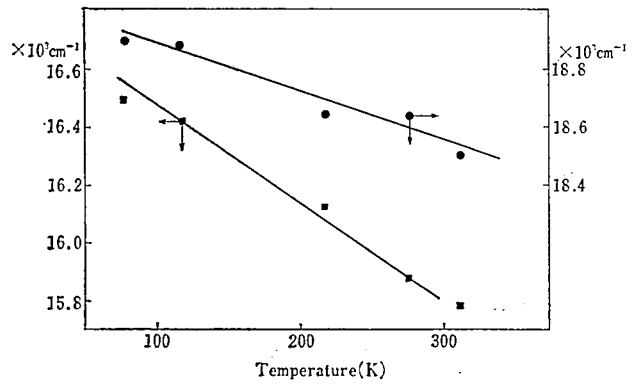

Fig. 9 Temperature dependences of the band position of $[Ti(urea)_6](ClO_4)_3$.

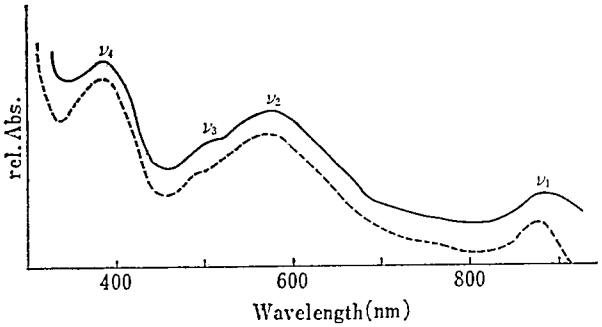

Fig. 10 Absorption spectra of $CsV(SO_4)_2 \cdot 12H_2O$, dotted line; 77K, solid line; 305 K.

Table 1 The values of the band maxima of $CsV(SO_4)_2 \cdot 12H_2O$.

Bands	Assignment	Absorption maxima (10^3 cm^{-1})	
		at 77K ($\times 10^3$ cm^{-1})	at 300K ($\times 10^3$ cm^{-1})
ν_1	$^1E_g, {}^1T_{2g} \leftarrow {}^3T_{1g}$ (F)	11.39	11.28
ν_2	$^3T_{2g}$(F) $\leftarrow {}^3T_{1g}$(F)	18.13	17.40
ν_3	$^1A_{1g} \leftarrow {}^3T_{1g}$ (F)	——	20.50
ν_4	$^3T_{1g}$(P) $\leftarrow {}^3T_{1g}$(F)	25.80	25.71

of ligand field parameters is carried out by using the energy matrices.[5] The values of B and Dq are as given below.

	at 77K	at 300K
B	597 cm^{-1}	643 cm^{-1}
Dq	1941 cm^{-1}	1874 cm^{-1}

The absorption spectrum of the hexaaquachromium (III) ions in $CrNH_4(SO_4)_2 \cdot 12H_2O$ had two absorption maxima at 17.53×10^3 cm^{-1} (ν_1) and 24.64×10^3 cm^{-1} (ν_2) as shown in Fig. 11. Hence the values of B and Dq are stated in the next page.

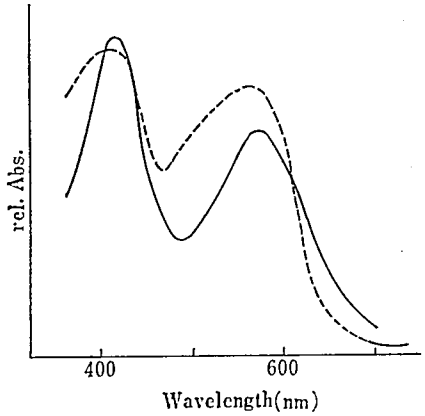

Fig. 11 Absorption spectra of $CrNH_4(SO_4)_2 \cdot 12H_2O$, dotted line; 77 K, solid line; 306~309 K.

	at 77K	at 300K
B	736 cm^{-1}	711 cm^{-1}
Dq	1816 cm^{-1}	1753 cm^{-1}

The crystal structure[6] of $MnSO_4 \cdot 4H_2O$ has not been accurately known except it is monoclinic. And in MnF_2 crystal six fluoride ions around the manganese ion are arranged in a pseudo-octahedron. Two of these six fluoride ions are at a distance 2.14 A from manganese ion and the remaining four at a distance 2.11 A. In a high-spin octahedral manganese (II) complexes all d-d bands must be due to spin-forbidden transitions. These too weak bands were shown in Fig. 12 and Fig. 13. The observed bands of $MnSO_4 \cdot 4H_2O$ and MnF_2 are assigned, as shown in Table 2. The absorption bands of $MnSO_4 \cdot 4H_2O$ crystal were shifted to the longer wavelength at low temperature and the values of Dq, B and C increased with decreasing temperature. No displacement, however, was found to occur by cooling MnF_2 down to 77K.

The spectra of hexaqua and hexammine-nickel complexes are illustrated in Fig. 14 and

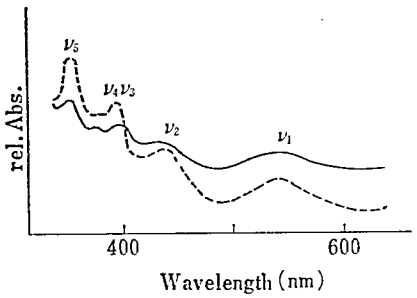

Fig. 12 Absorption spectra of $MnSO_4 \cdot 4H_2O$, dotted line; 77 K, solid line; 279~281 K.

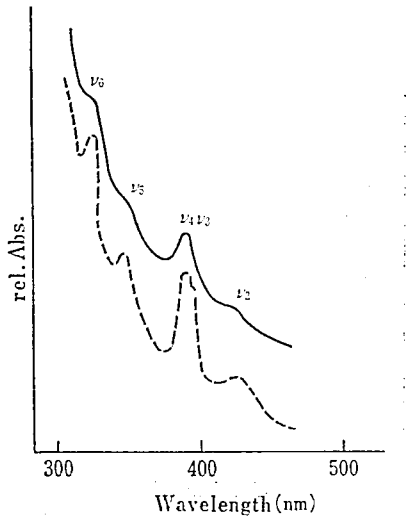

Fig. 13 Absorption spectra of MnF_2, dotted line; 77 K, solid line; 297 K.

Table 2 The positions of band maxima of $MnSO_4 \cdot 4H_2O$ and MnF_2.

Bands	Assignment	Absorption maxima		
		$MnSO_4 \cdot 4H_2O$		MnF_2
		at 77K	at 300K	
		($\times 10^3$ cm^{-1})	($\times 10^3$ cm^{-1})	($\times 10^3$ cm^{-1})
ν_1	$^4T_{1g}(G) \leftarrow {}^6A_{1g}$	18.24	18.76	——
ν_2	$^4T_{2g}(G) \leftarrow {}^6A_{1g}$	22.62	23.21	23.47
ν_3, ν_4	$^4A_{1g}, {}^4E_g \leftarrow {}^6A_{1g}$	25.03	25.13	25.33
ν_5	$^4T_{2g}(D) \leftarrow {}^6A_{1g}$	27.95	27.95	28.6
ν_6	$^4E_g(D) \leftarrow {}^6A_{1g}$	——	——	30.4

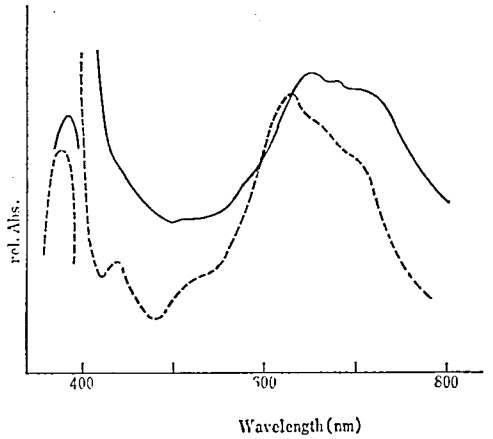

Fig. 14 Absorption spectra of $(NH_4)_2Ni(SO_4)_2 \cdot 6H_2O$, dotted line; 77 K, solid line; 284~286 K.

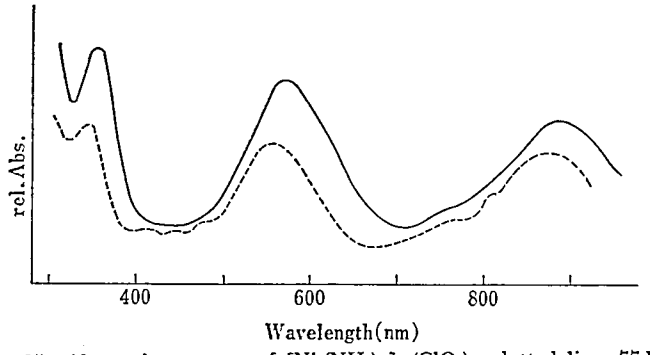

Fig. 15 Absorption spectra of $[Ni(NH_3)_6](ClO_4)_3$, dotted line; 77 K, solid line; 300 K.

Fig. 15. The ground state of nickel (II) in octahedral coordination is $^3A_{2g}(t_{2g})^6(e_g)^2$. Three absorption bands corresponding to the transitions.

$^3T_{2g}(F) \leftarrow {}^3A_{2g}$, $^3T_{1g}(F) \leftarrow {}^3A_{2g}$ and $^3T_{1g}(P) \leftarrow {}^3T_{2g}$.

should then be observed. The first band ($^3T_{2g}(F) \leftarrow {}^3A_{2g}$) of $(NH_4)_2Ni(SO_4)_2 \cdot 6H_2O$ in the infrared region could not be observed, because of limitation of the ability of a photo-

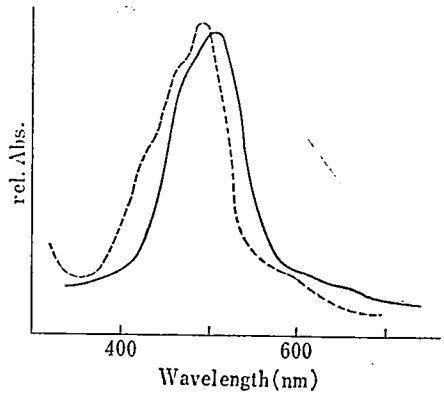

Fig. 16 Absorption spectra of $Co(NH_3)_2(SO_4)_2 \cdot 6H_2O$, dotted line; 77 K, solid line; 324~328 K.

multiplier.

For $[Ni(NH_3)_6](ClO_4)_2$, the five spin-forbidden absorption bands were located at 12.22×10^3 cm^{-1}, 13.39×10^3 cm^{-1}, 20.8×10^3 cm^{-1}, 22.7×10^3 cm^{-1} and 23.8×10^3 cm^{-1}. For $(NH_4)_2Ni(SO_4)_2 \cdot 6H_2O$ two bands were found at 19.2×10^3 cm^{-1} and 22.91×10^3 cm^{-1}. The values of B and Dq for $[Ni(NH_3)_6](ClO_4)_2$ are as following.

	at 77K	at 300K
B	960 cm^{-1}	1010 cm^{-1}
Dq	1105 cm^{-1}	1070 cm^{-1}

And for $(NH_4)_2Ni(SO_4)_2 \cdot 6H_2O$.

	at 77K	at 300K
B	880 cm^{-1}	884 cm^{-1}
Dq	971 cm^{-1}	848 cm^{-1}

Since Dq is inversely propotional to the 5th power of the interatomic distance between a metal ion and coordinated atoms, the increase of Dq can be explained by the contraction in volume with lowering temperature. Therefore, it is expected that B is decreased with decreasing temperature because the degree of covalency between a metal ion and coordinated atoms is increased by the decrease of a their interatomic distance.

Acknowledgements

One of us (Y.M.) is greatly indebted to, Professor M. Nakahara of Saint Pole's University, Professor S. Iwashima and Associate Professor R. Sato for their valuable discussions throughout this works.

We thank Mr. Takeda for the technicals provided for construction of the cryostat, and Mr. Yasuda, Mr. Nonaka, Mr. Ota, Mr. Ringo, Mr. Taga, Mr. Nagashima and Mr. Sato for a help in part of the measurements.

References

1) For example, O. G. Holmes and D. S. McClure, J. Chem. Phys., **26**, 1686, (1957).

2) B. Mayer, "Low Temperature Spectroscopy" p 119, Elsevier, (1971).
3) W. Kuhn and E. Braun, Z. Phys. Chem., **B8**, 281, (1930).
4) C. J. Ballhausen, "Introduction to Ligand Field Theory" p 99, McGraw-Hill Book Company, Inc., (1962).
5) Y. Tanabe and S. Sugano, J. Phys. Soc. Jpn., **9**, 753, (1954).
6) Edited by F. A. Cotton "Progress in Inorganic Chemistry" **10**, p 392, John Wiley & sons, Inc., (1968).